

availability of salt surfaces enriched in bromide, as also observed on freezing seawater in the Arctic (20), is a prerequisite for bromine release.

Typical temperatures at the Dead Sea were 40°C, about 40 to 60 K higher than in polar spring. Apparently the presence of ice surfaces, as often assumed, is not necessary to release bromine. At the Dead Sea, Br is most likely released by a heterogeneous autocatalytic process from the surface of the salt pans. A release from the sea surface or from aerosols formed by breaking waves is unlikely, as no bromine was observed when the wind came from the north, traveling over the Dead Sea itself. Extended salt pans are found in many other locations; even if the Br/Cl ratio is not high, a release of Br appears possible. It is not clear whether bromine from salt pans influences ozone concentrations only locally or on larger scales.

#### References and Notes

- J. W. Botzenheim, A. C. Gallant, K. A. Brice, *Geophys. Res. Lett.* **13**, 113 (1986).
- S. J. Oltmanns and W. D. Komhyr, *J. Geophys. Res.* **91**, 5229 (1986).
- R. P. Wayne *et al.*, *Atmos. Environ.* **29**, 2675 (1995).
- Active bromine and active chlorine are most likely released (17, 21) from sea salt deposits or sea salt aerosol, which normally contain (by weight) 55.7% Cl<sup>-</sup>, 0.19% Br<sup>-</sup>, and  $2 \times 10^{-5}$  % I<sup>-</sup>. Different heterogeneous release mechanisms have been proposed: (i) Reaction of nitrogen oxides (NO<sub>2</sub> or N<sub>2</sub>O<sub>5</sub>) with NaBr can form BrNO or BrNO<sub>2</sub>, which are easily photolyzed, forming Br (22). (ii) The oxidation by OH of the HBr that has been released from aerosols by acidification through H<sub>2</sub>SO<sub>4</sub> or HNO<sub>3</sub> is probably too slow to be important. (iii) An autocatalytic process may be important in which HOBr adsorbed on an acidic salt surface undergoes several reactions involving Br<sup>-</sup> (27, 23, 24). The Br<sub>2</sub> formed in these reactions is released into the gas phase and can be photolyzed and converted into two HOBr molecules. If <50% of the oxidized bromine is lost from the autocatalytic cycle, an effective release process will take place. This mechanism is suspected to occur on sea ice surfaces or in aerosol during Arctic spring (or both). Bromine atoms can also be formed by photolysis of alkyl bromides, such as CH<sub>3</sub>Br, emitted from algae in the ocean. This source is probably negligible in the Arctic spring and at the Dead Sea.
- M. Hausmann and U. Platt, *J. Geophys. Res.* **99**, 399 (1994).
- M. Tuckermann *et al.*, *Tellus* **49B**, 533 (1997).
- K. Kreher, P. V. Johnston, S. W. Wood, B. Nardi, U. Platt, *Geophys. Res. Lett.* **24**, 3021 (1997).
- A. Richter, F. Wittrock, M. Eisinger, J. P. Burrows, *ibid.* **25**, 2683 (1998).
- T. Wagner and U. Platt, *Nature* **395**, 486 (1998).
- U. Platt and J. Stutz, Eds., *HALOTROP Final Report* (University of Heidelberg, Heidelberg, 1998).
- U. Platt and C. Janssen, *Faraday Discuss.* **100**, 175 (1995).
- B. Alicke, K. Hebestreit, J. Stutz, U. Platt, *Nature*, in press.
- T. M. Niemi, Z. Ben-Avraham, J. R. Gat, Eds., *The Dead Sea, The Lake and Its Setting*, vol. 36 of *Oxford Monographs on Geology and Geophysics* (Oxford Univ. Press, New York, 1997).
- Dead Sea water is enriched in bromide by a factor of 70 relative to ocean water (0.07 g/liter<sub>water</sub> Br<sup>-</sup> in standard mean ocean water, 5 g/liter<sub>water</sub> in Dead Sea water).
- U. Platt and D. Perner, in *Optical and Laser Remote Sensing*, D. Killinger and A. Mooradian, Eds. (Springer-Verlag, New York, 1983), vol. 39 of *Springer Series in Optical Sciences*, pp. 95–105.
- The DOAS instrument used at the Dead Sea consists of two parts. A receiving Newtonian telescope ( $f = 1.8$  m, main mirror diameter 300 mm) was located in the van together with the spectrograph (0.5 m Czerny-Turner instrument, Spex 1870C, 600 g/mm) and a slotted disk spectral scanning device (5, 15, 17, 25) as detector. The xenon arc lamp (Osram XBO 450W/4) together with a transmitting telescope ( $f = 265$  mm, diameter 300 mm) was placed on the rooftop of a hotel 3.75 km south of the receiver. Spectra were recorded in the wavelength interval from 324 to 349 nm with a resolution of 0.25 nm. For the wavelength calibration of the detector-spectrograph system, the mercury emission line at 334.15 nm was recorded frequently. Atmospheric spectra were recorded with a 30-min time resolution. Background spectra were recorded within 5 min after each atmospheric spectrum to correct for scattered light in the atmosphere. Each spectrum was high-pass filtered by dividing by a fitted seventh-degree polynomial. Using a least squares method (78), we evaluated each spectrum by fitting three trace gas reference spectra. Spectra of O<sub>3</sub> and NO<sub>2</sub> were recorded by inserting a quartz cell filled with the respective gas into the light path; the BrO spectrum was created by degrading the literature spectrum of Wahner *et al.* (26) to our instrument function, yielding a differential absorption coefficient of  $\sigma' = 1.03 (\pm 0.1) \times 10^{-17}$  cm<sup>2</sup> for the 339-nm band.
- U. Platt, *Chem. Anal. Ser.* **127**, 27 (1994).
- J. Stutz and U. Platt, *Appl. Opt.* **35**, 6041 (1996).
- F. Ferlemann *et al.*, *Geophys. Res. Lett.* **25**, 3847 (1998).
- D. Wagenbach *et al.*, *J. Geophys. Res.* **103**, 10961 (1998).
- R. Vogt, P. J. Crutzen, R. Sander, *Nature* **383**, 327 (1996).
- B. Finlayson-Pitts and S. N. Johnson, *Atmos. Environ.* **22**, 1107 (1988).
- S.-M. Fan and D. J. Jacob, *Nature* **359**, 522 (1992).
- M. Mozurkewich, *J. Geophys. Res.* **100**, 199 (1995).
- F. Heintz, H. Flentje, R. Dubois, U. Platt, *ibid.* **101**, 891 (1996).
- A. Wahner, A. R. Ravishankara, S. P. Sander, R. R. Friedl, *Chem. Phys. Lett.* **152**, 507 (1988).

1 October 1998; accepted 18 November 1998

## Electrochemical Principles for Active Control of Liquids on Submillimeter Scales

Benedict S. Gallardo, Vinay K. Gupta,\* Franklin D. Eagerton, Lana I. Jong,† Vincent S. Craig, Rahul R. Shah,† Nicholas L. Abbott‡†

Electrochemical methods were combined with redox-active surfactants to actively control the motions and positions of aqueous and organic liquids on millimeter and smaller scales. Surfactant species generated at one electrode and consumed at another were used to manipulate the magnitude and direction of spatial gradients in surface tension and guide droplets of organic liquids through simple fluidic networks. Solid microparticles could be transported across unconfined surfaces. Electrochemical control of the position of surface-active species within aqueous films of liquid supported on homogeneous surfaces was used to direct these films into periodic arrays of droplets with deterministic shapes and sizes.

The development of simple and general principles for the pumping and positioning of liquids on submillimeter scales will enable fabrication of microanalytical instrumentation that would make procedures such as blood chemistry analysis, flow cytometry, polymerase chain reactions, and DNA screening both rapid and inexpensive (1). Current methods used to pump liquids within networks of channels, or to position liquids within arrays, generally rely on electrokinetic phenomena driven by high voltages (several kilovolts) (2), mechanical syringes and actua-

tors that are complicated to fabricate and too expensive to be disposable (3), or passive fluid phenomena such as capillary wetting (4). These methods are used to achieve largely serial manipulations of liquids (3) within permanent channels that direct the liquid motion (2–4). Here we report principles for the active control of liquids by the creation of gradients in surface pressure. In the same manner that changes in bulk solute concentration can lead to osmotic swelling (fluid transport), gradients in concentrations of molecules can lead to changes in surface tension that can be used to drive fluid motion. We created these gradients by using electrode surfaces to generate and consume surface-active species. This approach avoids the use of moving parts, uses low voltages (<1 V), permits vectorial transport and positioning of materials on unconfined surfaces, and can be applied to organic and aqueous liquids as well as solid microparticles. These methods make possible parallel manipulations of liq-

Department of Chemical Engineering and Materials Science, University of California, Davis, CA 95616, USA.

\*Present address: Department of Chemical Engineering, University of Illinois, Urbana, IL 61801, USA.

†Present address: Department of Chemical Engineering, University of Wisconsin, Madison, WI 53706, USA.

‡To whom correspondence should be addressed. E-mail: abbott@enr.wisc.edu

uids on surfaces that lack hydrophobic and hydrophilic patterns.

We used surface-active molecules (surfac-

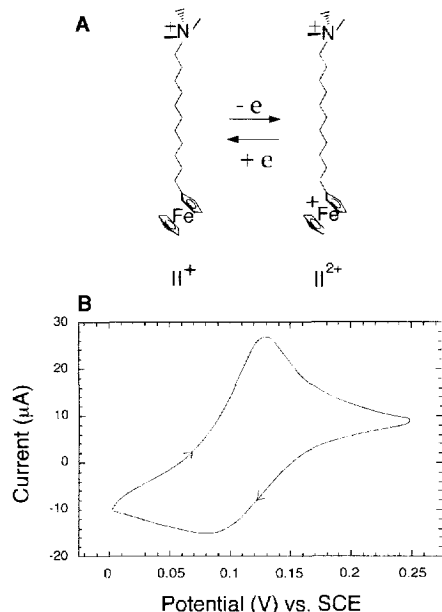


**Fig. 1.** (A) Redox-active surfactant  $\text{Fc}(\text{CH}_2)_{11}\text{N}^+(\text{CH}_3)_3\text{Br}^-$ :  $\text{II}^+$  (reduced) and  $\text{II}^{2+}$  (oxidized). (B) Cyclic voltammogram ( $20 \text{ mV s}^{-1}$ ) of an aqueous solution ( $0.01 \text{ M Li}_2\text{SO}_4$ , pH 1.3) of  $0.3 \text{ mM II}^+$ . See (17) for details.

tants) that incorporate redox-active groups (5). Whereas past uses of surfactants for passive control of liquids on surfaces have typically begun by dissolving a fixed and uniform concentration of surfactant into a solution (6), we used electrochemical methods to transform water-soluble molecules between surface-inactive ( $\text{II}^{2+}$ ) and surface-active states ( $\text{II}^+$ ) (Fig. 1) (7), and thereby achieved spatial and temporal control over the concentration of surface-active species in solution. We used this capability to actively control the motion and position of liquids by controlling the surface pressure exerted by molecules adsorbed at interfaces (8).

To demonstrate pumping of an organic liquid by use of the electrochemical transformation of  $\text{II}^+$  to  $\text{II}^{2+}$ , we fabricated a simple fluidic network consisting of four intersecting channels. Three of the channels ended at platinum (Pt) gauze electrodes that protruded through the surface of the solution, and the fourth channel ended at a reference electrode (saturated calomel electrode, SCE) and a Pt counterelectrode submerged beneath the surface of the solution. The fluidic network was filled with an aqueous solution of  $0.3 \text{ mM II}^{2+}$  to a depth of  $\sim 1 \text{ mm}$  (9). We pumped droplets of a nematic liquid crystal (LC) 4-*n*-pentyl-4'-cyanobiphenyl through the fluidic network because the LC is birefringent and

thus easily imaged through crossed polarizers. The application of oxidizing and reducing potentials of  $+0.3 \text{ V}$  and  $-0.3 \text{ V}$ , respectively, to any two of the three Pt electrodes in the network led to the pumping of LC droplets between those two electrodes (Fig. 2, A to C). The velocity of each droplet was controlled by the magnitude of the potential applied to the electrodes (Fig. 2D) (10).

The results of four experiments lead us to conclude that the pumping of the LC droplets is the result of electrochemically induced gradients in surface pressure maintained by the generation of surface-active species  $\text{II}^+$  at one electrode and consumption of  $\text{II}^+$  at the other electrode. First, the surface pressure of an aqueous solution of  $0.3 \text{ mM II}^{2+}$  increases by  $22 \text{ mN/m}$  upon reduction of  $\text{II}^{2+}$  to  $\text{II}^+$  (11). Second, we always observed the motion of the droplet to be directed away from the cathode and toward the anode, corresponding to motion in a direction of decreasing surface pressure (12). Third, we measured the onset of fluid motion to occur at a potential of  $\sim 0.1$

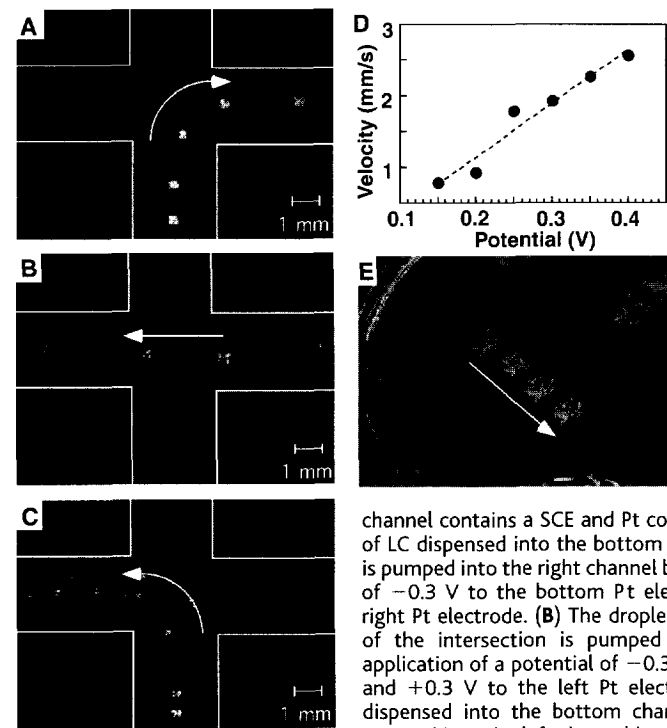


**Fig. 2.** Time-lapse images (left panels, four to six frames obtained at  $\sim 0.5 \text{ Hz}$ ) of the pumping of LC droplets across the surface of an aqueous solution of  $0.3 \text{ mM II}^{2+}$  ( $0.01 \text{ M Li}_2\text{SO}_4$ ) contained within a simple fluidic network formed by four glass microscope slides affixed to a larger glass plate. Platinum electrodes protrude through the surface of the solution at the ends of the left, right, and lower channels (widths  $\sim 4 \text{ mm}$ ). The end of the top

channel contains a SCE and Pt counterelectrode. (A) Droplet of LC dispensed into the bottom channel of the intersection is pumped into the right channel by application of a potential of  $-0.3 \text{ V}$  to the bottom Pt electrode and  $+0.3 \text{ V}$  to the right Pt electrode. (B) The droplet of LC in the right channel of the intersection is pumped into the left channel by application of a potential of  $-0.3 \text{ V}$  to the right Pt electrode and  $+0.3 \text{ V}$  to the left Pt electrode. (C) A droplet of LC dispensed into the bottom channel of the intersection is pumped into the left channel by application of a potential of  $-0.3 \text{ V}$  to the bottom Pt electrode and  $+0.3 \text{ V}$  to the left Pt electrode. (D) The velocity of fluid motion measured in a straight channel (width  $4 \text{ mm}$ ) as a function of applied potential. The x axis indicates the magnitude of the anodic and cathodic potentials. (E) Time-lapse image (four frames obtained at  $\sim 0.3 \text{ Hz}$ ) of sulfur microparticles supported on an unconfined surface of a solution of  $\text{II}^{2+}$ . Application of  $-0.3 \text{ V}$  to two Pt electrodes placed at the top and left sides of the image caused the sulfur microparticles to be pumped in the direction indicated by the arrow. The horizontal dimension of the image is  $\sim 40 \text{ mm}$ .

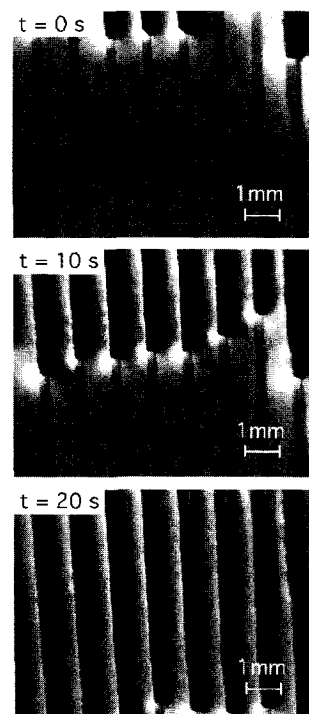


**Fig. 3.** Top views of the dewetting of an aqueous film of  $0.3 \text{ mM II}^+$  ( $0.01 \text{ M Li}_2\text{SO}_4$ , pH 1.3) supported on a microscope slide patterned with electrodes treated with gold. The electrodes were  $0.3\text{-mm}$ -wide parallel gold lines separated by  $1\text{-mm}$ -wide regions of glass. Dewetting was induced at the top edge of the microscope slide by application of  $0.5 \text{ V}$  (versus SCE) to the gold electrodes. The top panel ( $t = 0 \text{ s}$ ) shows a continuous film of liquid covering the electrodes (dark lines). Receding contact lines can be seen at the top of the image. The bottom two panels ( $t = 10$  and  $20 \text{ s}$ ) show retraction of the liquid across the surface at  $\sim 0.5 \text{ mm/s}$  (30). Liquid remains on the glass regions between the electrodes.

V, the half-wave potential for oxidation of  $\text{II}^+$  to  $\text{II}^{2+}$  (13). Fourth, application of oxidizing or reducing potentials in the absence of the redox-surfactant did not result in measurable fluid motion.

We also used electrochemical conversion of  $\text{II}^{2+}$  to  $\text{II}^+$  to transport particles across the unconfined surface of an aqueous solution. Whereas horizontal or vertical displacement of the suspended microparticles was observed to follow application of  $-0.3$  V to the left or top Pt electrode protruding through the surface of the solution shown in Fig. 2E, simultaneous application of  $-0.3$  V to both electrodes resulted in displacement of the microparticles in a direction given by the vector addition of the single-electrode flows.

To illustrate the use of redox-active surfactants for dispensing arrays of droplets on energetically homogeneous surfaces, we first patterned a surface with band electrodes by evaporating 50 Å of titanium and then 500 Å of gold onto glass microscope

slides through a micromachined aluminum mask. The surfaces of the electrodes were then derivatized by immersion in an ethanolic solution containing 0.9 mM 11-mercaptopundecanoic acid and 0.1 mM hexadecyl mercaptan for 30 min so as to make the entire surface energetically homogeneous (14). The patterned electrode surface was then inclined at  $\sim 20^\circ$  from the horizontal, with the lower edge touching a shallow pool of aqueous solution (0.01 M  $\text{Li}_2\text{SO}_4$ , pH 1.3) containing 0.3 mM  $\text{II}^+$ , a SCE, and a Pt counterelectrode. Surfactant solution was then applied by pipette onto the slide to form a continuous film [20 to 50  $\mu\text{m}$  in thickness (15)].

When an oxidizing potential (0.5 V versus SCE) was applied to the array of electrodes, the aqueous solution dewet the gold electrodes while the glass surfaces remained covered by liquid (Fig. 3) (16). The dewetting of the electrodes caused 1-mm-wide columns of liquid to form over the glass regions of the surface. With this procedure we created an array of  $\sim 100$  liquid droplets on a surface by using a mesh of electrodes (Fig. 4) (17). When no external potential was applied to the electrodes, a film of liquid supported on the surface was observed to drain uniformly from the surface (that is, no fluid pattern was formed). Also, patterned dewetting of an aqueous

film was not observed when  $\text{II}^{2+}$  or hexadecyltrimethylammonium bromide was used. We conclude that spatially localized changes in the concentrations of  $\text{II}^+$  and  $\text{II}^{2+}$  drive the formation of the pattern of liquid droplets (18). Because the pattern formed by the liquid could be prescribed by simply applying (or not applying) a potential to a specific electrode, a variety of different patterns could be formed on a given surface (19). Each surface could be used many times because a fresh supply of the active agent ( $\text{II}^+$ ) was delivered to the surface for each patterning event (20).

Whereas gradients in surface tension caused by reduction of  $\text{II}^{2+}$  to  $\text{II}^+$  drive the motion of liquid shown in Fig. 2, we do not believe gradients in surface tension can explain the direction of motion of liquid in Figs. 3 and 4. Oxidation of  $\text{II}^+$  to  $\text{II}^{2+}$  near the receding contact line of the solution in Figs. 3 and 4 would cause gradients in surface tension that lead to the spreading of a liquid across the surface and not dewetting of liquid, as we observed (21). We conclude that the motion of liquid shown in Figs. 3 and 4 is caused by an electrochemically induced increase in the contact angle of the solution on the surface. Young's equation,  $\cos\theta = (\gamma_{\text{SV}} - \gamma_{\text{SL}})/\gamma_{\text{LV}}$ , relates the equilibrium contact angle ( $\theta$ ) of a liquid on a solid to the interfacial free energies ( $\gamma_{ij}$ ) of the solid (S),

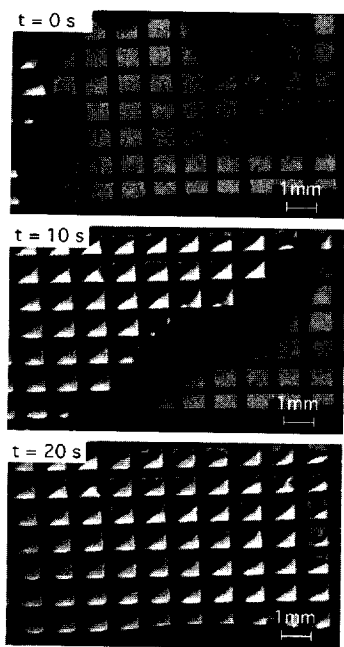
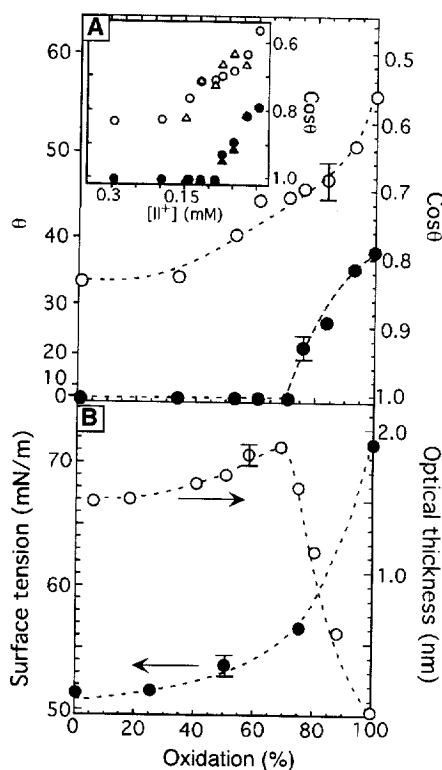


**Fig. 4.** Top views of the dewetting of an aqueous film of 0.3 mM  $\text{II}^+$  (0.01 M  $\text{Li}_2\text{SO}_4$ , pH 1.3) supported on a microscope slide patterned with a rectangular mesh of electrodes that was fabricated by the same procedures used to prepare the band electrodes shown in Fig. 3. Dewetting was induced at the top left corner of the microscope slide by application of 0.5 V (versus SCE) to the electrodes. The top panel ( $t = 0$  s) shows a continuous film of liquid covering the electrodes (mesh of dark lines). Receding contact lines can be seen at the left side of the image. The bottom two panels ( $t = 10$  and 20 s) show retraction of the liquid across the surface of the electrodes. Liquid droplets remain on the glass regions between the gold electrodes. The droplets were imaged with light incident from the lower right side of the images; the effects of shadowing create the diagonal lines that bisect each droplet.

**Fig. 5.** (A) Static advancing (open circles) and receding contact angles (filled circles) of aqueous solutions (0.01 M  $\text{Li}_2\text{SO}_4$ , pH 1.3) of 0.3 mM  $\text{II}^+$  plotted as a function of the extent of oxidation of  $\text{II}^+$  to  $\text{II}^{2+}$ . Contact angles were measured on the surface of treated films of gold. The inset shows advancing (open symbols) and receding (filled symbols) contact angles for partially oxidized solutions of 0.15 mM  $\text{II}^+/\text{II}^{2+}$  (triangles) and 0.3 mM  $\text{II}^+/\text{II}^{2+}$  (circles) plotted as a function of the concentration of  $\text{II}^+$  in solution. (B) Surface tensions ( $\gamma_{\text{LV}}$ , filled circles) and optical thicknesses (open circles) of surfactant adsorbed to treated gold as a function of the percentage oxidation of 0.3 mM  $\text{II}^+$  in aqueous 0.01 M  $\text{Li}_2\text{SO}_4$  at pH 1.3. The optical thickness was measured by using surface plasmon resonance reflectometry at 690 nm. Gold films (500 Å in thickness) were evaporated onto high index ( $n = 1.7925$ ) prisms (Applied Optics, Pleasant Hill, California) with an electron beam evaporator. The complex refractive index of the gold films at 690 nm was measured by spectroscopic ellipsometry to be  $0.1378 + i3.5661$ . The refractive index of the electrolyte solution containing 0.3 mM  $\text{II}^+$  was measured with an Abbe refractometer to be 1.3331 at 589 nm (23°C). The refractive index of the surfactant solution did not measurably change (to within  $\pm 0.0001$  refractive index units) when the aqueous solution of  $\text{II}^+$  was oxidized electrochemically to  $\text{II}^{2+}$ . The change in the absorbance of the solution was also confirmed to have a negligible influence on the surface plasmon reflectance. The change in position of the resonance minimum was modeled with either a four-layer (glass/gold/adsorbed surfactant/aqueous electrolyte) or five-layer (glass/gold/chemisorbed treatment layer/adsorbed surfactant/aqueous electrolyte) model by using a program written in Mathematica (31). The adsorbed surfactant layer was modeled as a layer having a refractive index of 1.45.



liquid (L), and vapor (V) phases (22). At equilibrium, no net force acts on the three-phase contact line of a liquid supported on a surface. An electrochemically induced increase in the local values of the interfacial free energies can, however, change the equilibrium contact angle from  $\theta_i$  to  $\theta_f$  and thus create a net force of magnitude  $\gamma_{LV}(\cos \theta_i - \cos \theta_f)$  that leads to motion of the contact line. Figure 5A shows that static contact angles (measured to be constant for times greater than 10 to 20 s) of aqueous solutions of 0.3 mM  $\text{II}^+/\text{II}^{2+}$  placed on the surface of treated gold do increase with oxidation of  $\text{II}^+$ . We conclude that the increase in contact angle is caused by a decrease in concentration of  $\text{II}^+$  and not an increase in concentration of  $\text{II}^{2+}$  for two reasons. First, advancing and receding contact angles measured at 100% oxidation of  $\text{II}^+$  are the same as for electrolyte solutions free of both  $\text{II}^+$  and  $\text{II}^{2+}$ . Second, contact angles of aqueous solutions of either 0.3 mM  $\text{II}^+/\text{II}^{2+}$  or 0.15 mM  $\text{II}^+/\text{II}^{2+}$  superimpose when plotted as a function of the concentration of  $\text{II}^+$  (inset in Fig. 5A) (23). The increase in receding contact angle (0.3 mM  $\text{II}^+/\text{II}^{2+}$ ) from  $<5^\circ$  to  $38^\circ$  coincides with a decrease in the amount of surfactant adsorbed at the liquid-solid interface, as measured by surface plasmon reflectometry (Fig. 5B). At 100% oxidation, no surfactant is adsorbed to the solid-liquid interface (24). This result strongly suggests that electrochemically induced desorption of surfactant from this interface [as well from the water-air interface (11)] plays a central role in causing the increase in receding contact angle, and thus the dewetting phenomena in Figs. 3 and 4. The treated gold surfaces at pH 1.3 are not significantly ionized (25). Adsorption of  $\text{II}^+$  is promoted by hydrophobic attraction between the surfactant and hexadecyl chains of the treated gold surface and opposed by electrostatic repulsion between the charges on the surfactants. The latter is increased for  $\text{II}^{2+}$  and drives its desorption at 100% oxidation (26).

Because the principles we report for patterned dewetting of liquids on surfaces rely on electrochemical control of the local concentration of surface-active species, the spatial resolution of these methods is influenced by the rate of lateral transport of  $\text{II}^+$  within a liquid film. For dewetting phenomena occurring over 1 to 10 s [millimeter-sized regions dewet at 1 mm/s (27)] and a surfactant diffusion coefficient of  $D \sim 10^{-6}$  cm<sup>2</sup>/s, we estimate the resolution of this method as  $R \sim (Dt)^{0.5} \sim 10$  to 30  $\mu\text{m}$ , a value that is comparable to the smallest features we formed in these experiments (28).

Our results demonstrate the usefulness of redox-active surfactants and electrochemical methods for active control of fluids on milli-

meter and smaller scales. When combined with electrochemical techniques widely used in detection schemes of analytical instrumentation (29), redox-active surfactants offer the possibility of designing highly integrated electroanalytical devices.

#### References and Notes

- K. Peterson, *Sens. Actuators A* **56**, 143 (1996); J. Fluitman, *ibid.*, p. 151; J. L. DeRisi, V. R. Iyler, P. O. Brown, *Science* **278**, 680 (1997).
- D. J. Harrison *et al.*, *Science* **261**, 895 (1993); H. Salimi-Moosavi, T. Tang, D. J. Harrison, *J. Am. Chem. Soc.* **119**, 8716 (1997).
- G. T. A. Kovacs, *Micromachined Transducers Sourcebook* (McGraw-Hill, Boston, 1998).
- E. Delamarche, A. Bernard, H. Schmid, B. Michel, H. Biebuyck, *Science* **276**, 779 (1997).
- Past studies have found redox-active surfactants to be compatible with a variety of analytes, including enzymes [P. Saudan *et al.*, *Biotechnol. Bioeng.* **44**, 407 (1994); D. M. Fraser, S. M. Zakeeruddin, M. Gratzel, *Biochim. Biophys. Acta* **1099**, 91 (1992)].
- B. Frank and S. Garoff, *Colloids Surf. A* **116**, 31 (1996), and references cited therein.
- Surfactant  $\text{II}^+$  was synthesized by procedures described previously [T. Saji, K. Hoshino, Y. Ishii, M. Goto, *J. Am. Chem. Soc.* **113**, 450 (1991)].
- The spreading of surfactant solutions over surfaces often leads to the creation of gradients in surfactant concentration; however, these gradients are passive and not under active control (6).
- Solutions of  $\text{II}^{2+}$  were prepared by oxidation of 0.3 mM solutions of  $\text{II}^+$  with about 1.0 equivalent of  $\text{Fe}^{3+}$  [as  $\text{Fe}_2(\text{SO}_4)_3 \cdot 5 \text{H}_2\text{O}$  (Aldrich)].
- We have also observed rapid, redox-induced spreading of micrometer-thick films of liquid across surfaces, thus demonstrating that rapid displacement of liquids across micrometer-thick films under surface pressure gradients induced by redox-active surfactants are possible.
- B. S. Gallardo, K. L. Metcalfe, N. L. Abbott, *Langmuir* **12**, 4116 (1996); D. E. Bennett, B. S. Gallardo, N. L. Abbott, *J. Am. Chem. Soc.* **118**, 6499 (1996). See also Fig. 5.
- Current passed at the anode was less than 100  $\mu\text{A}$  or  $\sim 1$  nmol of electrons per second. The velocity of migration of ions through the bulk of the 0.01 M solution of electrolyte was estimated to be  $<10$   $\mu\text{m/s}$ . We have also observed electrochemically induced Marangoni phenomena with concentrations of electrolyte of 0.1 M.
- Application of potentials greater than 0.5 V did not give rise to velocities of fluid motion greater than  $\sim 4$  mm/s. At these overpotentials, the rate-limiting step is likely to be mass transport to the electrodes (17).
- Advancing and receding contact angles of aqueous solutions used in our experiments were measured to be the same on surfaces of treated gold and glass (see Fig. 5).
- We used gravity to drain the film of liquid from the surface; other procedures, such as spin coating, can also be used to prepare a thin film of liquid.
- The direction of dewetting of the liquid was not governed by gravity. For example, we electrochemically induced motion of a contact line up an inclined surface. The motion of the contact line was typically initiated near the wire that connected the array of electrodes to the external circuit. This result suggests that the direction of dewetting is likely influenced by electric fields created by the applied external potential.
- Whereas the columns of liquid shown in Fig. 3 were permanent, the arrays of square droplets shown in Fig. 4 persisted for  $\sim 1$  min before respreading across the electrodes. Unlike the columns, the square droplets become electrically isolated from the counter electrode after formation. Electrical contact with droplets could, however, be maintained by patterning counter electrodes on surfaces. Arrays of droplets formed in this way would be permanent, as evidenced by the permanency of the liquid columns.
- Past studies of the patterning of aqueous solutions on surfaces have relied on the fabrication of surfaces that have hydrophilic and hydrophobic regions [N. L. Abbott, J. P. Folkers, G. M. Whitesides, *Science* **257**, 1380 (1992)] or regions that can be transformed electrochemically from hydrophobic to hydrophilic [N. L. Abbott, C. B. Gorman, G. M. Whitesides, *Langmuir* **11**, 16 (1995); C. B. Gorman, H. A. Biebuyck, G. M. Whitesides, *ibid.*, p. 2242]. The surfaces we used were not patterned with hydrophobic and hydrophilic regions.
- We individually addressed electrodes of the array shown in Fig. 3. The liquid only dewet the electrodes to which potentials were applied.
- Under conditions similar to those used in our experiments, the electrochemical response of gold electrodes derivatized with monolayers formed from  $\text{FcCO}(\text{CH}_2)_{15}\text{SH}$  was found to be limited to a few oxidation-reduction cycles because of the destruction of the molecules by side reactions [N. L. Abbott and G. M. Whitesides, *Langmuir* **10**, 1493 (1994)]. In contrast, we have observed reversible oxidation and reduction of  $\text{II}^+/\text{II}^{2+}$  in solution over  $\sim 1000$  cycles (B. S. Gallardo and N. L. Abbott, unpublished results).
- A. M. Cazaubert, F. Heslot, S. M. Troian, P. Carles, *Nature* **346**, 824 (1990); A. Carre, J.-C. Gestel, M. E. R. Shanahan, *ibid.* **379**, 432 (1996).
- T. Young, *Trans. R. Soc. London* **95**, 65 (1805).
- We have observed that  $\text{II}^{2+}$  lowers the surface tension of aqueous solutions at concentrations of  $\text{II}^{2+}$  greater than 0.3 mM (11).
- Ellipsometric measurements of the treated gold surface after dewetting of an oxidized solution of  $\text{II}^+$  revealed no adsorbed surfactant [K. Eskilsson and V. V. Yaminsky, *Langmuir* **14**, 2444 (1998)]. We did not observe stick-jump behavior of an advancing contact line at any concentrations of  $\text{II}^+$  or  $\text{II}^{2+}$  (6).
- K. Hu and A. J. Bard, *Langmuir* **13**, 5114 (1997).
- The optical thickness of the adsorbed layer of  $\text{II}^+/\text{II}^{2+}$  at the treated gold surface does not decrease monotonically with the extent of oxidation of  $\text{II}^+$ : A maximum is observed at  $\sim 70\%$  oxidation (Fig. 5B). We do not understand this behavior, although adsorption maxima have been reported in past studies of mixtures of surfactants that have widely varying critical micelle concentrations [J. Brinck and F. Tiberg, *Langmuir* **12**, 5042 (1996)].
- Hydrodynamic theory predicts a film of liquid to recede with velocity  $V \sim \gamma_{LV} \theta^3 / (288^{0.5} \eta L)$ , where  $\eta$  is the viscosity of the liquid, and  $L$  is a logarithmic factor of order 10 caused by divergence of the dissipation at the receding edge of the liquid [C. Redon, F. Brochard-Wyart, F. Rondelez, *Phys. Rev. Lett.* **66**, 715 (1991)]. Whereas the velocity of the electrochemically induced motion of the contact line in Figs. 3 and 4 is  $\sim 1$  mm/s, hydrodynamic theory predicts  $\sim 40$  mm/s for  $\gamma_{LV} = 50$  mN/m,  $\theta = 30^\circ$ , and  $\eta = 1$  mPa s. The lower experimental value is consistent with incomplete oxidation of  $\text{II}^+$  to  $\text{II}^{2+}$  within the film of liquid (as evidenced by the eventual respreading of drops in Fig. 4) and finite kinetics of adsorption-desorption of surfactant from the interfaces of the liquid film [H. Diamant and D. Andelman, *J. Phys. Chem.* **100**, 13732 (1996)].
- We have demonstrated patterned dewetting on surfaces with electrodes as small as 30  $\mu\text{m}$ .
- A. J. Bard, *Integrated Chemical Systems* (Wiley, New York, 1994).
- We observed the velocity of the contact line to vary between 0.5 and 1.0 mm/s from one experiment to the next. The variation in the velocity of the contact line likely reflects variations in the thicknesses of the liquid films.
- R. A. Dluhy, *J. Phys. Chem.* **90**, 1373 (1986).
- Partial support of this work was provided by the Camille and Henry Dreyfus Foundation, the David and Lucile Packard Foundation, the Donors of the Petroleum Research Fund, and the NSF (grants CTS-9410147 and CTS-9502263) and Office of Naval Research (PECASE award to N.L.A.). We thank A. Knoesen for helpful comments.

13 August 1998; accepted 13 November 1998